Study of the relationship between stacking fault energy and microstructure in different compositions of Fe-Mn steels produced by weld deposit

IOP Conf. Series: Materials Science and Engineering **668** (2019) 012001 doi:10.1088/1757-899X/668/1/012001

Study of the relationship between stacking fault energy and microstructure in different compositions of Fe-Mn steels produced by weld deposit

G G Ribamar[1,2], T C Andrade[1], H C Miranda[1] and H F G Abreu[1]

[1]Department of Metallurgical and Materials Engineering, Federal University of Ceará, Ceará, Fortaleza, Brazil

E-mail: giovanigoncalvesr@gmail.com

Abstract. The properties of high manganese steels are usually related to the mechanism of austenite deformation, either martensite or twin formation during deformation. This deformation mechanism is often related to the stacking fault energy (SFE) that the material possesses. Studies show that SFE values between 0 and 8 mJ/m² provide formation of ε martensite during deformation, whereas only twins are formed for energies above 18 mJ/m². Intermediate values provide the formation of both ε martensite and twins. In this way, it is possible to predict the microstructure and, consequently, mechanical properties with the knowledge of the material's SFE. In this work, a weld consumable with high manganese content was deposited on a SAE 1012 carbon steel plate with the flux-cored arc welding process producing different chemical compositions and consequently different SFE that varied as a function of the dilution. Low dilution conditions led to austenite and ε martensite formation in the molten zone, while in high dilution conditions, α' martensite were found, besides those other two. Manganese was found to be the most influential element in the phase formation change, based on SFE and SFE components analysis.

1. Introduction

High manganese steels are alloys with outstanding mechanical properties due to the activation of deformation mechanisms such as twins or martensite formation [1]. Steels with manganese content higher than 15 wt.% have shown to be excellent materials for automotive and cryogenic applications, because of their good ductility and strength combination, besides the stabilization of austenite at room temperature, avoiding the ductile-fragile transition at low temperatures [2]. Nowadays, it is well known the relation between deformation mechanism and the stacking fault energy (SFE) in high manganese steels. For those with low SFE values, ε and/or α' martensite tend to form during their deformation, increasing its strength by hard phase formation, effect called transformation induced plasticity (TRIP) [3]. On the other hand, for those steels with high SFE values, the increase in the strength accounts for twin formation inside austenite phase, effect called twinning induced plasticity (TWIP) [3].

The main reason for these effects is due to the stabilization level of austenite which increase with the manganese and carbon content [4]. Xiong *et al.* (2014) showed the influence of these elements on the SFE, demonstrating that, at SFE values close to 0 mJ/m², ε martensite has formed even without any deformation, while at higher SFE this martensite was formed just after some deformation level, or

even did not formed [4]. Curtze *et al.* (2010) have studied the dependence of tensile deformation behavior on SFE, temperature, and strain, showing that austenite becomes more stable with the increase in temperature [5]. Besides, they showed that the magnetic component is strongly affected by temperature, being the main reason to austenite stabilization [5].

The SFE can be calculated based on model proposed by Olson and Cohen [6] as follows:

$$SFE = 2\rho\Delta G^{\gamma\rightarrow\epsilon} + 2\sigma^{\gamma/\epsilon} \quad (1)$$

where ρ is the molar surface density for the $\{111\}_\gamma$ closed packed planes, $\Delta G^{\gamma\rightarrow\epsilon}$ is the molar Gibbs energy for $\gamma \rightarrow \varepsilon$ phase transformation and $\sigma^{\gamma/\epsilon}$ is the energy per surface unit of the $\{111\}$ interface between the γ and ε boundary. The molar Gibbs energy is dependent of two components: chemical and magnetic Gibbs free energy, $\Delta G_{che}^{\gamma\rightarrow\epsilon}$ and $\Delta G_{mg}^{\gamma\rightarrow\epsilon}$ respectively, and can be calculated as follows:

$$\Delta G^{\gamma\rightarrow\epsilon} = \Delta G_{che}^{\gamma\rightarrow\epsilon} + \Delta G_{mg}^{\gamma\rightarrow\epsilon} \quad (2)$$

Although development has been made in this area, it is difficult to find studies on welding with filler metal for these steels. The main works in this field are limited to autogeneous welding, such as friction stir welding [7], resistance spot welding [8], and high frequency electrical resistance welding [9]. One of the reasons for this absence is due to its composition sensitivity, because a little change in manganese or carbon content can affect the austenite deformation mechanism [10], leading to a very strong decreasing in steel's properties. In order to understand it, the present work aims to study SFE/microstructure relationship using different high manganese steels made by weld deposit. It was used a high manganese filler metal and a SAE 1012 plate steel as base metal through the flux cored arc welding (FCAW) process. The steel compositions were measured by energy dispersive spectroscopy (EDS) and the microstructures were obtained using a scanning electronic microscopy (MEV). The SFE and SFE components were calculated and related to dilution and microstructure obtained.

2. Materials and Methods

2.1. Welding

The different steels were made using FCAW process. A high manganese steel electrode as consumable and an SAE 1012 steel as base metal were used. The different steels obtained were taken from the weld zone. The chemical composition of the materials is shown in Table 1. The different steels were obtained varying the weld dilution level, which was calculated using the geometric method [11]. Table 2 shows the welding parameters used.

Table 1. Materials Chemical composition. All values are in wt.%.

	Mn	Ni	Cr	Si	C	Fe
PT-400HM	20.94	3.76	0.87	0.58	0.17	Bal.
SAE 1012	0.60	-	-	-	0.12	Bal.

Table 2. Welding Parameters.

	Power (W)	Current (A)	Tension (V)	Welding Speed (cm/min)	Feed rate (m/min)	Energy (kJ/mm)
B-11	7480	220	34	15	10	3.0
B-07	7480	220	34	22	10	2.0
A-31	7480	220	34	30	10	1.5
A-38	7480	220	34	45	10	1.0

2.2. Characterization

Steels characterization were carried out using standard metallography procedures, which involved grinding with silicon carbide papers, followed by polishing with diamond suspensions, and finally,

polishing with colloidal silica for several hours in order to avoid martensite presence due to sample preparation. The samples were etched with a 10% Nital solution (10% Nitric Acid + 90% Alcohol) and the structure was observed with SEM. EDS measurements were carried out in a SEM using 20 kV and working distance of 10 mm.

2.3. Stacking Fault Energy

The SFE were calculated following Equation 1. The equation developments can be found in references [4,6,10]. All functions and constants can be found in [5, 12-22].

3. Results and Discussion

Different dilution values were obtained varying the welding speed, forming four different alloys, as can be seen in Table 2. Figure 1 shows scanning electron micrographs of all four steels and the Table 3 shows the chemical composition, SFE values calculated from this composition, dilution level and microhardness values. DuPont (2011) found the similar result for a stainless austenitic steel [23], although the materials are quite distinctives, the arc physics is the same. The microstructure for all steels shows dendritic morphology, with epitaxial grains. For alloys A-38 and A-31, those who achieved high dilution level, α' martensite and austenite/ε martensite were found, while for alloys B-11 and B-07, just austenite phase was present. Besides, twins can be seen in A-31, B-11, and B-07 conditions.

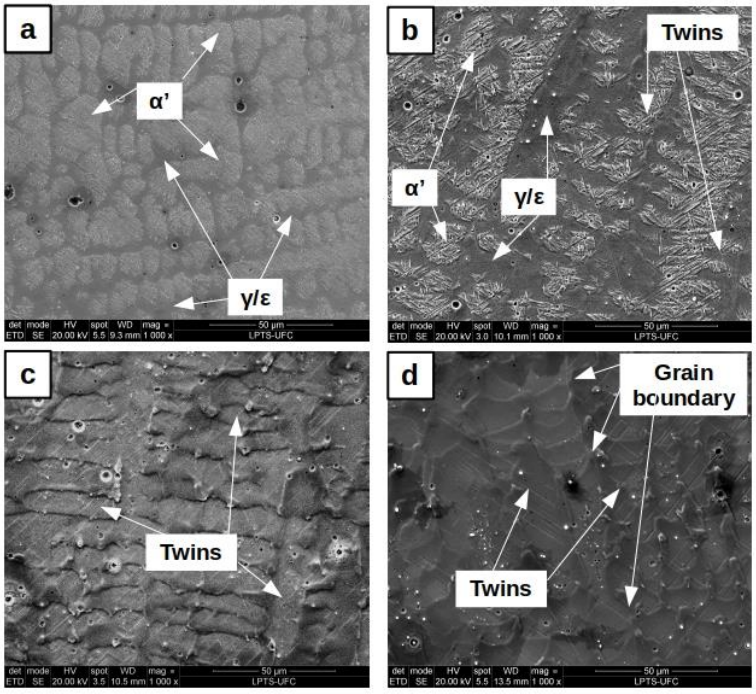

Figure 1. Scanning electron micrographs of alloy (a) A-38, (b) A-31, (c) B-11, and (d) B-07.

The dendritic morphology is more apparent in steels with α' martensite, because it is formed in the core of dendrite. During the solidification process, manganese is rejected and the poor manganese regions transform into α' martensite, while the inter dendritic spaces do not, due to their higher manganese content. Comparing A-38 and A-31, the presence of α' martensite decrease. The lower dilution level leads to a higher manganese content in weld zone (Table 3), which provide more regions of austenite stabilized. B-11 and B-07 conditions

do not show α' martensite presence and the manganese condition measured is higher than 18 wt.%. For those conditions with higher dilution level, A-31 and A-38, calculated SFE values showed to be negative, while for those with lower dilution, just austenite twinned were observed. Besides extend works about SFE/microstructure relationship [1, 3, 24, 25], no mention has been made about negative SFE and α' martensite presence. The α' martensite absence in low dilution conditions is reflected in microhardness values, which decrease with the decreasing in dilution level, that is, with the α' martensite fraction decrease. The high standard deviation occurs due the manganese microssegregation that increase the hardness by solid solution or even by α' phase transformation, leading to different hardness values.

Table 3. Chemical composition, SFE, dilution level and microhardness values obtained from all conditions.

Condition	Mn	C	Ni	Si	Cr	Fe	SFE (mJ/m²)	Dilution (%)	Hardness (HV)
A-38	12.69	0.15	2.05	0.32	0.51	Bal.	-5.1	37.7	346 ± 12.5
A-31	14.69	0.15	2.66	0.51	0.59	Bal.	-1.0	31.1	269 ± 18.5
B-11	18.71	0.16	3.42	0.50	0.82	Bal.	7.1	11.3	242 ± 20.0
B-07	18.91	0.17	3.42	0.54	0.76	Bal.	7.4	7.6	225 ± 18.5

Although the hardness value has been decreased with the decrease in α' martensite fraction, the austenite TRIP or TWIP effect can be present, leading to high strength with higher ductility. Curtze et al. (2010) and Xiong et al. (2015) showed the deformation mechanism influence on the high manganese mechanical properties [5, 26], where martensite formation rose the work hardening rates, while it decreased the ductility. Then, a balance of α' martensite and austenite can be predicted by dilution level for these two materials (base metal and filler metal). Despite the authors do not found a clear evidence of the composition limit to α' martensite formation, it was found in SFE values. In order to understand it, influence of dilution level on the SFE value was calculated, as well as on the chemical and magnetic Gibbs free energy component, as can be seen in Figure 2a.

Figure 2a shows the relation between dilution level and SFE, magnetic, and chemical Gibbs free energy. The markers point out SFE calculated from the steel's composition, showed in Table 3. The values fit very well with the curves obtained for the base and filler metal studied. The SFE value decreased with the increasing in dilution level, as well as the chemical Gibbs component (Figure 2a). However, the magnetic component appears to have little influence on the total Gibbs Free energy, decreasing smoothly with the increase in dilution. The increase in dilution level refers to a change in more than one element [11], and so, it is important to analyze carefully the chemical composition of the two weld materials in order to obtain a good understanding of the dilution influence on the SFE, and consequently, on the microstructure developed.

Figure 2b shows manganese influence on the SFE and its components. The composition calculated was the filler metal composition, varying just manganese content. It can be seen the strong manganese influence on the SFE, passing easily for all fields of phase transformation and twin formation presented by [2, 24], who presented the phase prediction based on the chemical composition of manganese and carbon. Although their diagram has shown a good tool for phase prediction in high manganese steels, additional elements such as nickel, silicon and chromium are not considered. Overcoming this problem, thermodynamic SFE model shows a better tool, enabling additional elements consideration and other ways to use this tool,

as the one used in the present work, with dilution level. As thermodynamic SFE's main components are the chemical and magnetic Gibbs free energy, they can show useful information to understand the SFE increasing behavior. For manganese, both chemical and magnetic component increase, leading to a high increasing in SFE value. On the other hand, nickel does not show an increase in magnetic component, despite of SFE increase with nickel addition. Similar results were found by Xiong et al. (2014) [4], however, no mention was made about nickel influence. Both manganese and nickel are austenite stabilizers, with nickel being the most influential (Figures 2b and 2c). However, the high nickel cost justifies the manganese preference.

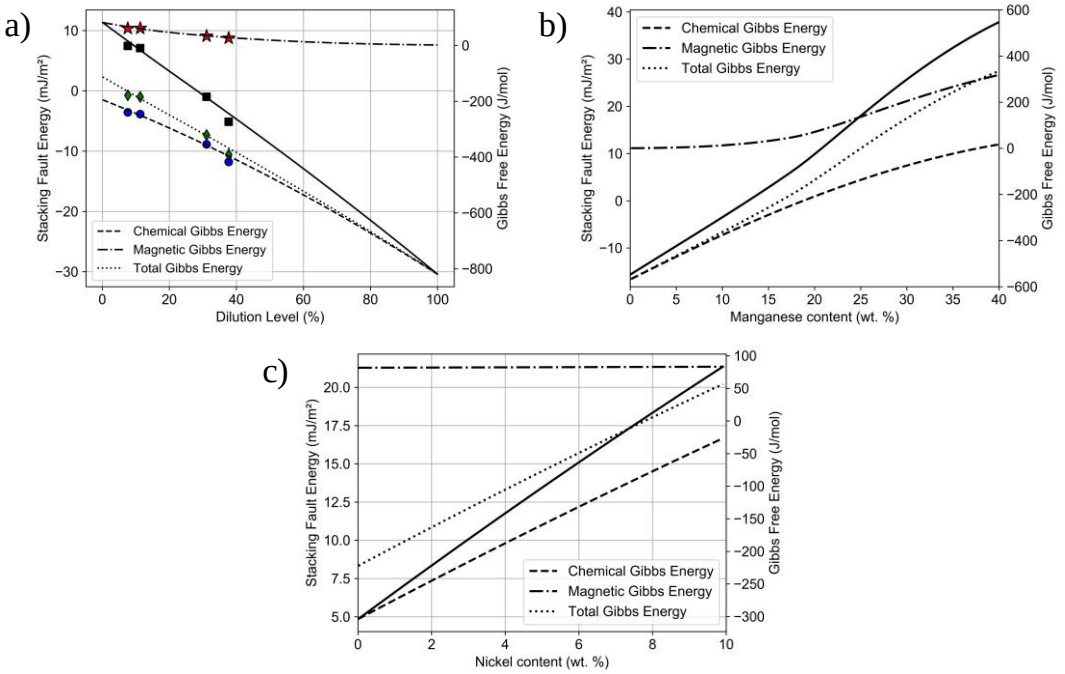

Figure 2. SFE, ΔG, dilution relationship, and (b) Manganese, (c) Nickel influence on SFE and ΔG. Squares, circles, stars and diamonds corresponds to SFE, chemical, magnetic and total Gibbs free energy measured for the four alloys, respectively.

The results showed a good relation achieved between dilution, SFE and microstructure. Negative SFE values led to α' martensite formation, while positive SFE values did not. Manganese was the most influential element to increase SFE value, because it was the element with the most composition difference between base and filler metal, and because manganese increases both magnetic and chemical Gibbs free energy component.

4. Conclusions

It was obtained four high manganese steels by welding deposit. The chemical composition, microstructure and stacking fault energy was studied and related with dilution level. The following statement can be drowned from the results:

- The increasing in welding speed led to a higher dilution level, and consequently high α' martensite formation and microhardness value;

- The dendritic morphology led to regions with high α' martensite density and others with austenite/ε martensite. The reason for this morphology accounts for the manganese microssegregation, what increased the standard deviation in microhardness;
- SFE calculated in function of dilution level showed a smooth decrease in magnetic Gibbs free energy component, while a rapid decreasing in chemical component were found. It led to a continuous decreasing in SFE value with the increase in dilution level;
- Manganese was the major influential element in the SFE value, due to increase both chemical and magnetic Gibbs free energy component and for the high chemical difference between base and filler metal.

Acknowledgements
This study was financed in part by the Coordenação de Aperfeiçoamento de Pessoal de Nível Superior - Brasil (CAPES) - Finance Code 001.

References
[1] De Cooman B C, Kwon O and Chin K G 2012 *Mater. Sci. Technol.* **28** 513-27
[2] Choi J K, Lee S G, Park Y H, Han I W and Morris Jr J W 2012 High manganese austenitic steel for cryogenic applications *22nd International Offshore and Polar Engineering Conference* (South Korea: Technical Research Laboratories) pp 29-35
[3] De Cooman B 2017 *High Mn TWIP steel and medium Mn steel Automotive Steels* (Amsterdam: Elsevier) pp 317-85
[4] Xiong R, Peng H, Si H, Zhang W and Wen Y 2014 *Mat. Sci. Eng. A-Struct.* **598** 376-86
[5] Curtze S and Kuokkala V T 2010 *Acta Mater.* **58** 5129-41
[6] Olson G B and Cohen M 1976 *Metall. Trans. A* **7** 1897-904
[7] Li Y j, Fu R d, Li Y, Peng Y and Liu H j 2018 *J. Mater. Sci. Technol.* **34** 157-62
[8] Paveebunvipak K and Uthaisangsuk V 2018 *Mater. Design* **160** 731-51
[9] Park G, Jeong S, Kang H and Lee C 2018 *Mater. Charact.* **139** 293-302
[10] Curtze S, Kuokkala V T, Oikari A, Talonen J and Hanninen H 2011 *Acta Mater.* **59** 1068-76
[11] DuPont J N and Marder A R 1996 *Metall. Mater. Trans. B* **27** 481-9
[12] Dinsdale A 1991 *Calphad* **15** 317-425
[13] Ishida K 1976 *Phys. Status Solidi A* **36** 717-28
[14] Ishida K and Nishizawa T 1974 *Trans. Japan Institute of Metals* **15** 225-31
[15] Dumay A, Chateau J P, Allain S, Migot S and Bouaziz O 2008 *Mat. Sci. Eng. A-Struct. A* **483-484** 184-7
[16] Yang W S and Wan C M 1990 *J. Mater. Sci.* **25** 1821-3
[17] Chen S, Chung C, Yan C and Hsu (Xu Zuyao) T 1999 *Mat. Sci. Eng. A-Struct. A* **264** 262-8
[18] Adler P H, Olson G B and Owen W S 1986 *Metall. Trans. A* **17** 1725-37
[19] Allain S, Chateau J P, Bouaziz O, Migot S and Guelton N 2004 *Mat. Sci. Eng. A-Struct. A* **387-389** 158-62
[20] Yakubtsov I, Ariapour A and Perovic D 1999 *Acta Mater.* **47** 1271-9
[21] Wu X and Hsu (Xu Zuyao) T 2000 *Mater. Charact.* **45** 137-42
[22] Zhang Y S, Lu X, Tian X and Qin Z 2002 *Mat. Sci. Eng. A-Struct. A* **334** 19-27
[23] Dupont J N 2011 *Dilution in Fusion Welding Welding Fundamentals and Processes* vol 6A (ASM International) pp 115-21
[24] De Cooman B 2012 *Phase transformations in high manganese twinning-induced*

plasticity (TWIP) steels Phase Transformations in Steels vol 2 (Amsterdam: Elsevier) pp 295-331
[25] De Cooman B C, Estrin Y and Kim S K 2018 *Acta Mater.* **142** 283-362
[26] Xiong R, Peng H, Wang S, Si H and Wen Y 2015 *Mater. Design* **85** 707-14